



ELSEVIER

Available online at www.sciencedirect.com

SCIENCE @ DIRECT®

Engineering Structures 28 (2006) 668–681

ENGINEERING
STRUCTURES

www.elsevier.com/locate/engstruct

Dynamic identification of a reinforced concrete frame in progressive states of damage

Zbigniew Zembaty^{a,*}, Marcin Kowalski^a, Stanislav Pospisil^b

^a Faculty of Civil Engineering, Technical University of Opole, 45-233 Opole, ul. Mikolajczyka 5, Poland

^b Institute of Theoretical and Applied Mechanics, Czech Academy of Sciences, Prosecka 7, Praha 9, Czech Republic

Received 6 October 2004; received in revised form 26 September 2005; accepted 26 September 2005

Available online 23 November 2005

Abstract

Two, full size, reinforced concrete frames were put on a shaking table and underwent seismic excitations with increasing intensities. The aim of the reported experiment was to study changes in their dynamic, modal parameters due to development of cracks in concrete. Dynamic identification of these frames was carried out through diagnostic tests interlaced with the damaging excitations. This paper presents the results of their identification in various states of damage, using low level non-destructive damage estimation methods. A characteristic decrease of natural frequencies and an increase of structural damping was observed. The drop of the natural frequency was fastest for the 1st mode and slower for the further modes. It was noted that the loss of natural frequencies equaled about 10% and still the first cracks could not be visually detected (loss of stiffness 15%). The advantages and disadvantages of the application of a shaking table for modal analyses of full size, civil engineering structures are pointed out in detail.

© 2005 Elsevier Ltd. All rights reserved.

Keywords: Structural dynamics; Identification; Modal analysis; Damage assessment; Reinforced concrete; Cracks

1. Introduction

Reinforced concrete (r/c) structures are often exploited as partly cracked. Typical examples are r/c bridges for which the cracks develop gradually from the moment when they are erected as the result of sudden overloading, seismic effects (e.g. [21]), corrosion, excessive temperature effects etc. There is also an opposite phenomenon as concrete strength increases over many years after casting (see e.g. [3]). As an effect the actual, overall elastic properties of r/c structures are difficult to predict. Since some of the r/c structures have suddenly crumbled or had to be put out of operation without an early warning, the problems of Non-destructive Damage Evaluation (NDE) of these structures become more and more important. During the last 20 years methods of system identification and modal analysis developed into quite a large interdisciplinary field, [7,12], covering also the NDE problems. For example for the rotating machines it is now routine to detect their damage

even without taking them out of service (e.g. [20]). However practical application of these methods for large engineering structures met some difficulties (see Los Alamos state of the art reports — by Doebling et al. [6] and Sohn et al. [17]). In spite of this, the search for implementation of these methods continues (see e.g. the state of the art review by Salawu [16]). For the reinforced concrete structures it started as early as in the fifties of the 20th century [15], but more experimental research took place from the early eighties. For example, Wang et al. [19] experimented with impact tests on small beams (61 cm) with various boundary conditions. They noted a 25% drop of the natural frequencies and a substantial increase of structural damping. Maeck and De Roeck [11] investigated 6 m long r/c beams after statically imposed damage at several levels. They included an analysis of the curvature of the beams as well as investigations of bending and reduction of torsional stiffness with the developed damage. They noted a drop of stiffness reaching 50% and 40% for bending and torsional stiffness respectively. Recently Ndambi et al. [14] carried out an analysis also of 6 m long r/c beams but with the general aim of localizing the statically inflicted damage. They studied the applicability

* Corresponding author. Fax: +48 77 4 566 124.

E-mail address: zet@po.opole.pl (Z. Zembaty).

of classic modal damage indicators like MAC — Modal Assurance Criterion (see Eq. (3)) and COMAC (Coordinate MAC). Although the MAC could reveal the symmetry or asymmetry in the damage location and COMAC might help to detect and localize the damage more precisely, effects such as the damage severity and spreading were difficult to reflect. Ndambi et al. [14] found that the damage indices such as the strain energy methods are very promising in damage monitoring, but concluded that still the frequency drop seemed to be the best measure of damage severity.

The purpose of this paper is to report the results of an experiment on a reinforced concrete structure tested on a MASTER shaking table in CESI-ISMES, Bergamo, Italy. Unlike the research mentioned before, the examined structure was a 12 ton frame vibrating in two dimensions in the horizontal plane. The structure was subjected to distributed damage due to progressively increasing inertial loads applied by kinematic motion of the shaking table. Though such an approach excluded any detailed studies of localization effects it enabled us to investigate dynamic behavior of full scale r/c structures in various damage states in the laboratory environment.

2. Statement of the problem

Consider the familiar, linear dynamic equation of motion of discrete dynamic systems

$$\mathbf{M}\ddot{\mathbf{q}} + \mathbf{C}\dot{\mathbf{q}} + \mathbf{K}\mathbf{q} = \mathbf{F}(t) \quad (1)$$

in which matrices \mathbf{M} , \mathbf{C} and \mathbf{K} stand for the matrices of inertia, damping and stiffness respectively, $\mathbf{q} = \mathbf{q}(t)$ is the vector of system displacements and $\mathbf{F}(t)$ stands for the vector of external forces exciting the structure. A typical purpose of linear structural identification is to find the properties of a dynamic system described by matrices \mathbf{M} , \mathbf{C} , \mathbf{K} given the measured response vector \mathbf{q} and excitation vector \mathbf{F} . In reality, due to the non-uniqueness of the inverse problem, a reduced set of parameters describing the structural properties is searched for. Typical examples of such identifications are modal models described by a limited number of natural modes, their damping ratios and modal participation factors.

Consider now the equations of the eigenproblem

$$\mathbf{M}\ddot{\mathbf{q}} + \mathbf{K}\mathbf{q} = \mathbf{0} \quad (2a)$$

$$\det(\mathbf{K} - \omega^2\mathbf{M}) = 0 \quad (2b)$$

$$(\mathbf{K} - \omega_i^2\mathbf{M})\mathbf{w}_i = \mathbf{0}. \quad (2c)$$

In its simplest form the identification problem deals with the relationship between the matrices of inertia and stiffness on the one side and solutions of the eigenproblem i.e. natural frequencies ω_i [rad/s], f_i [Hz] and eigenvectors \mathbf{w}_i on the other side. While it is a simple matter to calculate the natural frequencies and eigenvectors from the known matrices \mathbf{M} and \mathbf{K} it is more difficult to deduce about the changes in matrix \mathbf{K} by observing the variations in the natural frequencies and eigenvectors which is the subject of dynamic identification and damage detection. To quantify differences between analytical and experimental mode shapes as well as between respective

mode shapes of intact and damaged structures, the so-called Modal Assurance Criterion (MAC) was proposed (e.g. [7,12]). It can be obtained by calculating the following formula:

$$\text{MAC}(i, j) = \frac{\left(\sum_{k=1}^{k_{\max}} w_{ki}^{(a)} w_{kj}^{(e)} \right)^2}{\left(\sum_{k=1}^{k_{\max}} w_{ki}^{(a)} w_{ki}^{(a)} \right) \left(\sum_{k=1}^{k_{\max}} w_{kj}^{(e)} w_{kj}^{(e)} \right)} \quad (3)$$

in which superscript (a) over the mode “ w ” describes an analytical, natural mode, while superscript (e) describes a respective experimental mode. The formula (3) can also be used to compare mode shapes of intact and damaged structures.

The analyses of the elastic properties of reinforced concrete structures revealed that due to inherent cracks appearing during their exploitation the variations of effective stiffness of r/c structural members can be quite substantial. Early experiments by Franz and Brenner in 1967 [9] or recent theoretical investigations by Jędrzejczak and Knauff in 1997 [10] proved that from the intact state, when concrete beams under bending behave linearly, until they are considered damaged, the loss of their stiffness may reach 50% to 60%. Such substantial variations in their effective elastic properties make the r/c structures particularly convenient for assessing their properties by measuring forced, low level vibrations and, in particular, by observing changes in their natural frequencies and eigenvectors. The experiment described in this paper aimed at studying such dependence between dynamic properties of a r/c structure and its damage states.

3. Description of the experiment

Figs. 1 and 2 present a photograph and general view of one of the two reinforced concrete frames under investigation. The two frames were designed as identical, 415 cm high, with the columns fixed in the lower spandrel beams. The horizontal overall dimensions of each structure equaled 340×340 cm with one symmetry axis along the x direction. The frame was built of two types of columns with rectangular cross-sections 20×20 cm and 20×40 cm with main reinforcing bars $\varnothing 10$ mm and stirrups made of bars $\varnothing 8$ mm (Fig. 3). The distance of the stirrups equaled 15 cm at the 90 cm upper and lower sections of the columns and 30 cm in the mid-section (see photo in Fig. 4). The thickness of the upper r/c slab equaled 15 cm. Total mass of each frame equaled about 12 tons. For this type of frame three basic natural mode shapes of lateral vibrations can be distinguished:

- two translations along x and y axes
- and torsion about vertical axis z .

In addition, higher natural modes of vibration, representing single motions of columns, can be observed. However, as was revealed for these frames by FEM analyses, such modes were over 60 Hz frequency and presented a minor contribution in structural response. To properly separate the first three natural frequencies, a special, additional mass was mounted off-center, on the top of the slab (see Fig. 2). Both r/c frames, denoted



Fig. 1. Photograph showing one of the analysed r/c frames on the shaking table.

here as *frame no. 1* and *frame no. 2*, were erected in the main CESI-ISMES experimental hall. After 28 days each frame was transported on the shaking table and fixed by bolts $\text{\O}50$ mm with distance 30 cm. Concrete samples from both frames were taken during casting and subjected to standard tests for compressive strength. The frames were instrumented using accelerometers A1–A16 as well as displacement transducers W1–W15 measuring the strain of the columns.

The dynamic analyses started from a set of diagnostic, low level tests on intact frame no. 1:

- First the frame was subjected to impulse loads.
- Next the sweep-sine resonance tests were done by the shaking table.
- Next white noise excitations were carried out.
- Finally respective low level seismic excitations were done, for which an artificially generated accelerogram of an earthquake was applied (Fig. 5).

After the intact structure was extensively examined, a series of seismic tests with increasing intensity was carried out. This was done by applying the same seismic signal multiplied by an increasing factor which resulted with shaking table excitations with peak (ground) accelerations (PGA) from about $0.15g$ to $1.1g$ ($g = 9.81 \text{ m/s}^2$). The damaging tests were interlaced with low level diagnostic tests described above. The acceleration records chosen for both damaging and diagnostic excitations were simulated to represent a broad-band seismic spectrum (see Fourier spectra from Fig. 5).

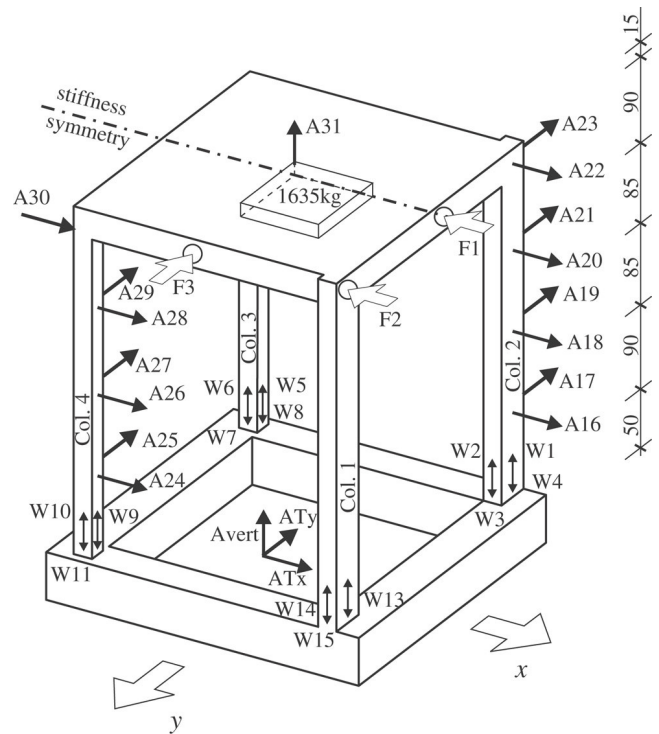


Fig. 2. General view of the analysed frame(s) with the locations of accelerometers (A), displacement transducers (W), and places where impulse loads were exerted (F).

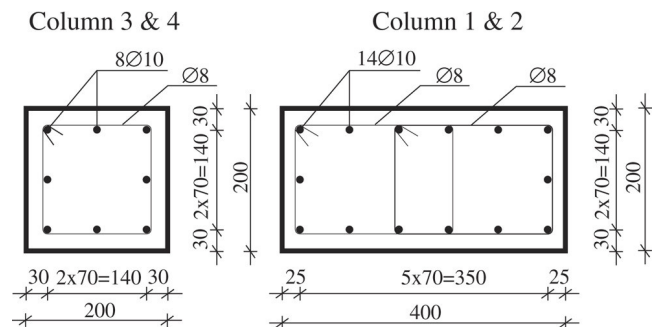


Fig. 3. Cross-sections of columns of the analysed frames.



Fig. 4. Detail of the reinforcement.

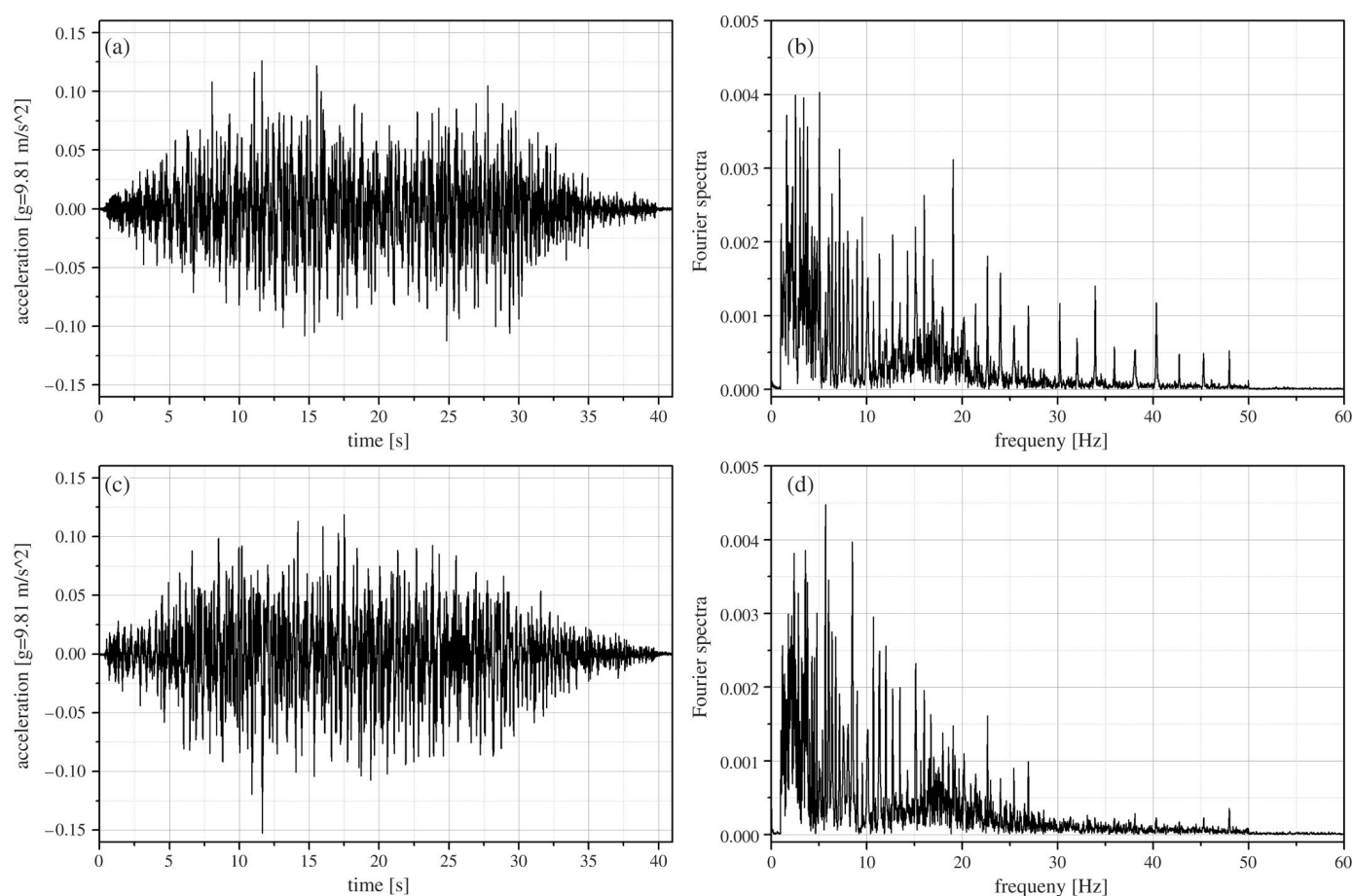


Fig. 5. Seismic records of accelerations along x and y axes (a, c) and their Fourier spectra (b, d) applied to damage the frames and for diagnostic purposes.

4. CESI-ISMES “MASTER” shaking table

The CESI-ISMES “MASTER” shaking table is a 4×4 m platform of welded steel plates which can move in 6 degrees of freedom (3 translations — x , y , z and 3 rotations about these axes). A mechanism of 8 actuators driven by oil pumps and a partially automatic control system allows the table to reach maximum overturning moment of 300 kNm and maximum mass of specimen statically compensated equal to 50 tons. However, for controlled dynamic tests the mass of the tested specimen should be lower. The actual maximum peak accelerations possible to achieve depend on the model mass and geometry, as well as on the time history to reproduce. The most difficult problem for all 6-dofs shaking tables is how to ensure proper reproduction of the required time history for heavy models which may cause substantial vibration interaction with the vibrating platform. This problem is called table–model interaction and is similar to the well known soil–structure interaction effect. The strongest, unwanted effect to deal with is the spurious rocking appearing in the vibrations of the model–table system. The mass of the specimen in this experiment was equal to 12 tons and its height of about 4 m was not substantial so there was no problem for the control software of the table to properly reproduce the applied accelerogram without inducing any rocking. However, since the mass of the vibrating parts of the shaking table equals about 11 tons

(shaking platform and actuators) which is almost the same as the mass of the specimen, the dynamic system representing the specimen and the table was introducing substantial, additional damping coming from the actuators. This damping cannot be compensated for, unless the ratio of the mass of the specimen and shaking table is substantially low.

5. Identification techniques

The main purpose of the experiment was to investigate changes in the dynamic properties of the model structure using *low level*, diagnostic excitations or ambient vibrations. That is why the identification techniques were chosen from the classic, linear methods, suitable to apply during or before shaking table experiments:

5.1. Impact tests

The impact tests were done using a wooden beam hanging on an overhead crane so the resulting impulses were not measured, but they were kept rather small. The points where the impacts were exerted are denoted as F1–F3 in Fig. 2. The damping coefficient was calculated from these records of free vibrations which displayed clear, single mode responses. The calculations were carried out directly from the measured decay rate [4].

$$\xi \approx \frac{a_n - a_{n+j}}{2\pi j a_{n+j}} \quad (4)$$

where a_n and a_{n+j} denote the amplitude after n cycles and $n + j$ cycles respectively. It should be noted that unlike for the other methods of identification the damping obtained during impact tests was not affected by the bias from table–structure interaction. Next the Fourier transforms of the free vibration signals were computed to obtain the resonance frequencies by the peak picking technique.

5.2. Sweep-sine tests

The sweep-sine tests were carried out by kinematic, harmonic motion of the shaking table in one, selected horizontal (x, y) direction. The amplitude of the harmonic accelerations equaled about $0.05g$. During the tests the frequency of excitation was slowly increasing from 0.5 Hz until 70 Hz. The amplitudes and phases from all the sensors were recorded. When the harmonic excitations were reaching natural frequencies the vibrations of the frame displayed respective natural modes. These vibrations were however too fast and too small to be visually observed, but they could be retrieved from the recorded phases and amplitudes. For this purpose a special program was written in the *Matlab* language. It displayed on a computer screen animated vibrations of the frames in respective resonances. In addition the natural modes retrieved from sweep-sine tests can quantitatively be compared with the analytical ones (Eq. (2)) or between the damaged and intact ones, using the MAC coefficient (Eq. (3)). The damping ratios were obtained from plots of the modulus of the transfer functions by applying the familiar method of half power bandwidth [4].

5.3. Random tests

Another test aiming at retrieving the transfer function of the structure (transmittance) was carried out by exciting low level, band limited white noise vibrations of the shaking table along selected horizontal directions. The test lasted several minutes so that steady state, stationary vibrations were excited, during which it was possible to observe “on line” the shape of the transfer function $H_{q_i u}(\omega)$, from the following formula [2]:

$$H_{q_i u}(\omega) = \frac{S_{q_i u}(\omega)}{S_u(\omega)} \quad (5)$$

in which $S_{q_i u}(\omega)$ is the co-spectral density of the signal measured for excitation channel u and response channel q_i , while $S_u(\omega)$ is the respective auto spectrum of the excitation process and ω is angular frequency [rad/s]. The analysed, stationary structural response was analysed in time windows of duration 10.24 s from which the spectral densities were obtained by time averaging. The natural frequencies were observed by peak picking and respective damping ratios were calculated by applying the half-power bandwidth method.

5.4. Dynamic identification from time history response and excitation records (seismic tests)

Consider a structure under two-component, horizontal excitations (Fig. 6). The equation of motion of this structure

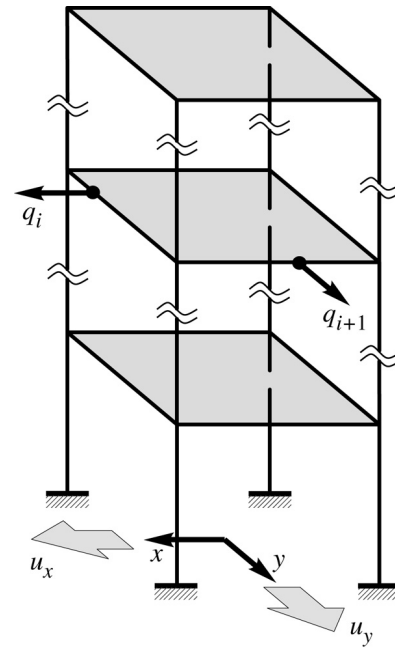


Fig. 6. A structure under two-component seismic excitation.

discretized by applying FEM techniques takes the following form:

$$\mathbf{M}\ddot{\mathbf{q}} + \mathbf{C}\dot{\mathbf{q}} + \mathbf{K}\mathbf{q} = -\mathbf{M}\mathbf{r} \begin{Bmatrix} \ddot{u}_x(t) \\ \ddot{u}_y(t) \end{Bmatrix} \quad (6)$$

in which $u_x(t)$ and $u_y(t)$ are the horizontal components of excitation and \mathbf{r} is the special influence matrix

$$\mathbf{r} = \begin{Bmatrix} \dots & \dots \\ \dots & \dots \\ 1 & 0 \\ 0 & 1 \\ \dots & \dots \\ \dots & \dots \end{Bmatrix} \begin{matrix} i \\ i + 1 \end{matrix} \quad (7)$$

with elements in the first column equal to 1 for degrees of freedom parallel to the x axis and 0 for the perpendicular ones. Analogously the second column contains unit elements for the degrees of freedom parallel to the y axis and 0 for the perpendicular. For example, in the above equation q_i is parallel to the x axis and q_{i+1} is parallel to the y axis.

Introducing the modal transformation and applying Fourier transforms makes it possible to present the response of the i -th dynamic degree of freedom as a sum of contributions from each vibration mode and both excitations:

$$Q_i(\omega) = A_l(\omega) + \omega^2 \sum_{k=1}^{\infty} \beta_{ix}^k H_k(\omega, \omega_k, \xi_k) A_x(\omega) + \omega^2 \sum_{k=1}^{\infty} \beta_{iy}^k H_k(\omega, \omega_k, \xi_k) A_y(\omega), \quad (8)$$

where $l = \begin{cases} x & \text{for } q_i \parallel x \\ y & \text{for } q_i \parallel y \end{cases}$

Table 1
Concrete properties and dynamic characteristics of intact frames

	Compressive concrete strength (MPa)	Young's modulus of concrete (MPa)	f_1 (Hz) direction x	f_2 (Hz) direction y	f_3 (Hz) torsion
Frame no. 1	32.76	30 248	4.81	5.89	10.47
Frame no. 2	36.65	31 527	4.88	5.98	10.58

where $Q_i(\omega)$ is the i -th response in the frequency domain, β_{ix}^k , β_{iy}^k are the effective modal participation factors, $A_x(\omega)$, $A_y(\omega)$ are the Fourier transforms of the excitation accelerations and

$$H_k(\omega) = \frac{1}{\omega_k^2 - \omega^2 + 2i\xi_k\omega_k\omega} \quad (9)$$

is the frequency response function of the k -th mode of vibration.

The effective modal coefficient β_{ix}^k describes the actual contribution of excitation along the x axis in the vibrations of the i -th co-ordinate (i -th measuring channel) vibrating in the k -th mode. Analogously the coefficient β_{iy}^k is a measure of the contribution of excitation along the y axis in the vibrations of the i -th co-ordinate vibrating in the k -th mode.

Eq. (8) defines the modal model. There are four parameters to identify for each mode k :

- natural frequency ω_k ,
- modal damping ratio ξ_k and
- two effective modal participation factors β_{ix}^k and β_{iy}^k .

To identify all three dominating modes of the analyzed frame $4 * 3 = 12$ parameters will have to be computed. The identification can be performed by minimizing the mean square difference between Fourier transforms of measured signals ${}^m Q_i(\omega)$ and responses $Q_i(\omega)$ calculated in terms of Fourier transforms of excitations $A_x(\omega)$, $A_y(\omega)$, using Eq. (8). This can be done by minimizing the following functional:

$$J = \int_{\omega_b}^{\omega_e} |Q_i(\omega) - {}^m Q_i(\omega)|^2 d\omega. \quad (10)$$

The minimization of functional (10) can be done by applying a classic quasi-Newton approach together with the search in one dimension, the Davidon–Fletcher–Powell algorithm: [5,8]. This method requires the initial approximation and gradient vector to be calculated in every step of the routine. Transforming the response given by Eq. (8) back to the time domain (Eq. (11)) gives the actual response time history which can be compared with the measured response:

$$x(t) = \frac{1}{2\pi} \int_{-\infty}^{+\infty} X(\omega) e^{i\omega t} d\omega. \quad (11)$$

The identification method described above is based on classic approaches developed by Beck [1] and McVerry [13]. Detailed derivation of the extension of this method to 2D kinematic excitations can be found in the paper by Zembaty and Kowalski [22] together with its application to identification of masonry structures subjected to shaking table excitations. The above algorithm for “seismic” identification of structures was implemented as Fortran code.

Table 2
Values of MAC coefficient for experimental vs. analytical modes of intact frame 2

	Analytical modes			
	1	2	3	
Experimental modes	1	0.9999	0.0177	5.53E-4
	2	0.0135	0.9278	0.0073
	3	5.28E-4	0.1162	0.9999

Table 3
Damping ratio of intact frames

	From free vibrations along direction x ξ	From free vibrations along direction y ξ	From free torsional vibrations ξ
Frame no. 1	1.81%	–	1.95%
Frame no. 2	–	2.15%	–

6. Results of tests for intact frames

In Tables 1–3 results of the tests of intact frames are shown. Table 1 shows concrete strength and Young's modulus as well as resonance frequencies measured during impact tests. It can be seen from this table that as the concrete of the second frame is stronger and has a greater Young's modulus value, the respective natural frequencies, as could be expected, are shifted by about 2% in accordance with the respective ratios of the square roots of E . The presence of at least three horizontal accelerometers on the upper slab made it possible to obtain images of the mode shapes from sweep-sine tests by applying a specially written for this purpose *Matlab* program, described earlier. In Figs. 7–11 these mode shapes are shown as excited by kinematic motions along the x and y axes. It can be seen that the stiffness symmetry along the x axis results in an almost symmetrical mode along the x axis. On the other hand, the differences in symmetry with respect to the y axis resulted in the pendulum-like shape of the second natural mode. Obviously the excitations along the y axis more clearly excited the second natural mode. The torsional resonance motion was obtained from both directions of excitations. The *Matlab* generated animations of these modes were compared with their respective eigenmodes generated by FEM. In Table 2 a MAC comparison (Eq. (3)) between experimental and analytical mode shapes is shown for frame 1. A very good match could be observed both from the animations and MAC matrix. Table 2 indicates however some small coupling between the 2nd (along the y axis) and the 3rd (torsional) mode.

Table 3, in turn, presents respective damping ratios obtained from free vibrations during impact tests and calculated by

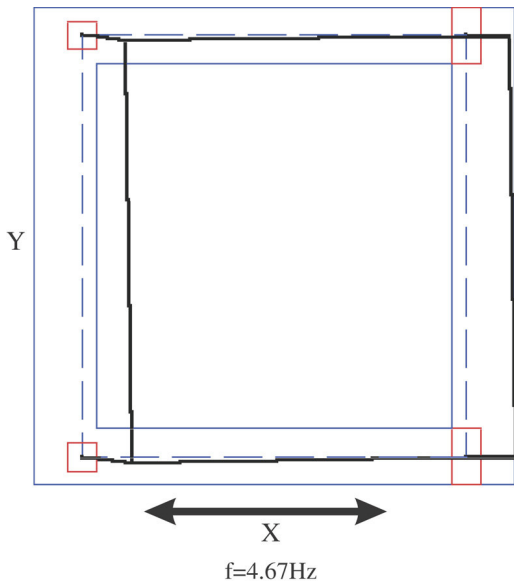


Fig. 7. Shape of the first natural mode (in intact state) identified from sweep-sine tests with excitation along the x direction.

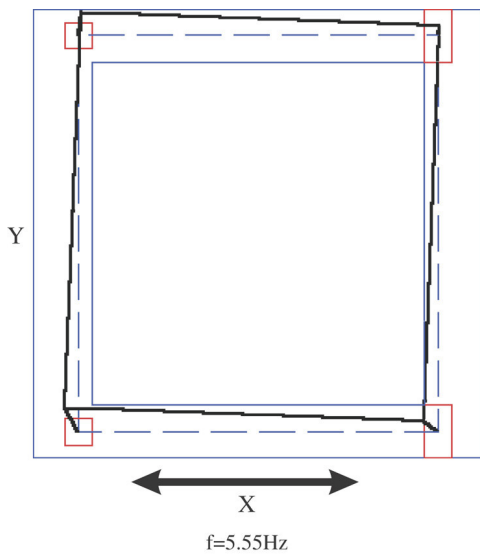


Fig. 8. Shape of the second natural mode (in intact state) identified from sweep-sine tests with excitation along the x direction.

Eq. (4), in cases when single mode, free vibrations could clearly be detected. The maximum accelerations of the upper slab during these free vibrations equaled about 40 cm/s^2 and 0.02 cm of displacements. The time domain window covering j peaks for Eq. (4) was shifted along the time axis and the differences in the obtained damping ratio were negligible. The damping ratios of about 2%, typical for r/c structures, are noted.

The application of identification from time history records of excitation and response led to the results shown in Fig. 12. A good match between the response measured and computed (Eq. (8)) can be seen. The identification process ended after 93 iterations of the minimization algorithm.

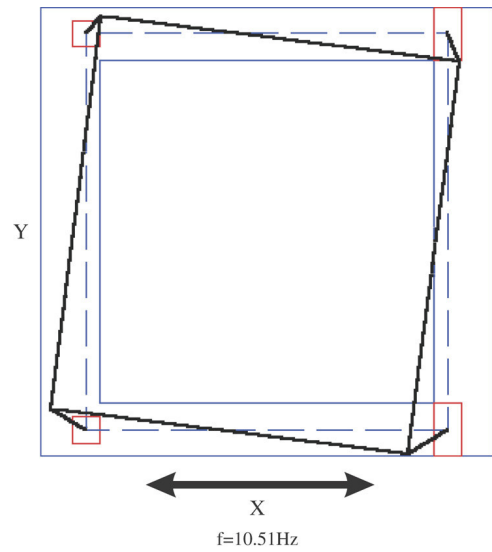


Fig. 9. Shape of the third natural mode (in intact state) identified from sweep-sine tests with excitation along the x direction.

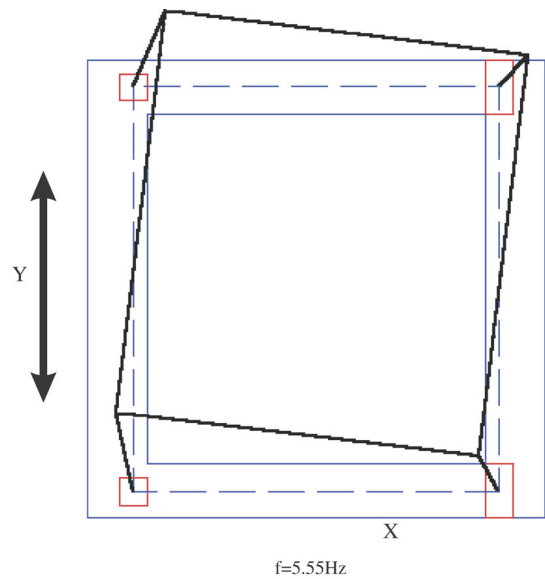


Fig. 10. Shape of the second natural mode (in intact state) identified from sweep-sine tests with excitation along the y direction.

7. Frames under progressive damage

Each state of damage inflicted by the strong motion excitations was followed by an inspection and careful documentation of the eventual cracks which were marked on the concrete surface using different color markers depending on the level of excitations. Next these damages were drawn in the special protocols. In Figs. 13–17 the protocols of the damage for column no. 2 of frame 2 are shown as an example. Characteristic, dominating distance between cracks of 15 cm can be seen. It equals the distance between respective stirrups. In Fig. 18 a photograph displaying damaged detail and color-marked cracks is shown. After each inspection of damage, low level, diagnostic excitations (as for the intact frame) were

Table 4
Consecutive phases of damage for frame no. 2

Level of excitation and damage		<i>MM</i> intensity	Description of damage
Damage state	Signal amplification Peak horizontal accel./velocity		
“N” not damaged	–12 dB PGA = 35.6 cm/s ² PGV = 1.63 cm/s	III + (3.37)	Intact frame
State I	0 dB PGA = 142 cm/s ² PGV = 6.08 cm/s	VI – (5.65)	No visible damage
State II	6 dB PGA = 319 cm/s ² PGV = 11.2 cm/s	VII – (6.72)	First, horizontal cracks are observed. For columns with greater cross-section only at the lower spandrel beams, for columns with smaller cross-section the cracks are visible also at the upper part
State III	9 dB PGA = 413 cm/s ² PGV = 16.9 cm/s	VII + (7.44)	Existing cracks are developed. New cracks appear in the upper part of columns with greater cross-sections
State IV	12 dB PGA = 654 cm/s ² PGV = 23.8 cm/s	VIII (8.02)	Further development of the existing cracks. Extensions of upper and lower crack zones. Average distance between cracks about 15 cm (the same as the distance between stirrups).
State V	(14 dB) PGA = 843 cm/s ² PGV = 29.3 cm/s	VIII + (8.39)	Further propagation of existing cracks and appearance of inclined cracks
State VI	(16 dB) PGA = 1090 cm/s ² PGV = 38.2 cm/s	IX – (8.85)	Small parts of concrete are falling, exposing the reinforcement in the upper parts of columns

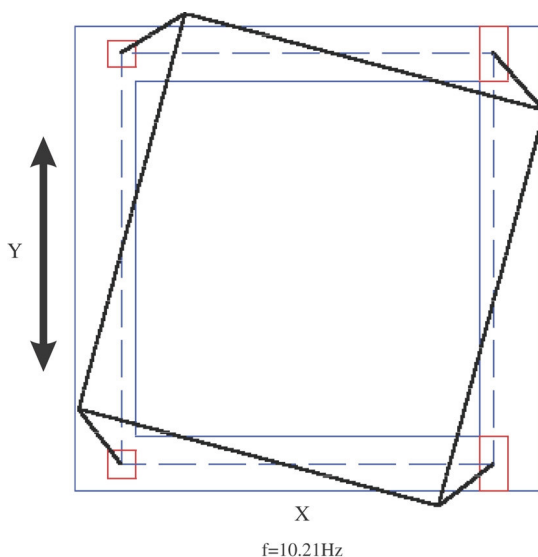


Fig. 11. Shape of the third natural mode (in intact state) identified from sweep-sine tests with excitation along the *y* direction.

carried out to investigate the changes done to modal properties of the frame. The cycle of interlaced strong and low level excitations ended when the frame was substantially damaged. A similar program of tests was carried out with minor changes for frame no. 2. In the case of the second frame experience gained during the first experiment was taken into account. The damage sequence of frame number 1 revealed a need to add an intermediate level of damaging excitations before the first cracks appeared. However the final test results as

obtained in various states of damage did not differ between both frames. But since for the second frame one additional damage level was included then all the results shown in this paper refer to frame no. 2 unless stated otherwise. In Table 4 the detailed sequence of the tests of frame no. 2 is shown and explained. To describe better the excitations reached at the shaking table at various damage levels Table 4 includes maximum accelerations (PGA) and velocities (PGV) obtained as horizontal maxima i.e. $\max \sqrt{x^2 + y^2}$, and an assessment of Modified Mercalli (*MM*) intensity obtained on the shaking table. For the earthquake with broad-band spectrum and long duration (Fig. 5) a good match between *MM* intensity (I_{MM}) and peak velocity (v) can be obtained. Using the Trifunac and Brady [18] formula: $\log_{10} v = 0.25I_{MM} - 0.63$, [$v = \text{cm/s}$], respective *MM* intensities were calculated (numbers in parentheses) and rounded to full values expressed in Roman numbers, with +/- signs displaying slightly lower or greater values.

In Figs. 19–21 the plots of frequency response functions as obtained from different accelerometers during random tests are shown for various levels of inflicted damage. As more and more cracks were appearing, the natural frequencies were getting lower and lower. Accelerometer A22 parallel to the *x* axis displays only the changes in the first natural frequency. On the other hand the frequency response function obtained from accelerometer A23 parallel to the *y* axis shows changes of both the second mode along the *y* axis and the 3rd torsional mode. This is due to lack of symmetry in stiffness with respect to the *y* axis and from small coupling of the 2nd mode with torsion (see MAC value from Table 2). It is however interesting

Table 5
Selected natural frequencies of frame no. 2 identified during tests: “random”, “sweep-sine” and “seismic” (description of damages I–VI: Table 4 and Figs. 13–17)

State	Random				Sweep-sine				Seismic			
	f_1 (Hz) A22 x	A30 x	f_2 (Hz) A23 y	f_3 (Hz) A23 y	f_1 (Hz) A22 x	A30 x	f_2 (Hz) A23 y	f_3 (Hz) A23 y	f_1 (Hz) A22 x	A30 x	f_2 (Hz) A23 y	f_3 (Hz) A23 y
N	4.69	4.69	5.32	10.16	4.67	4.67	5.55	10.16	4.45	4.47	5.14	9.69
I	4.20	4.20	4.98	9.77	3.92	3.92	4.80	9.23	3.96	3.96	4.72	9.10
II	2.83	2.83	3.61	7.42	2.46	2.46	3.20	6.86	2.49	2.49	3.30	–
III	2.44	2.44	3.22	6.54	2.07	2.07	2.82	5.89	2.09	2.10	2.84	–
IV	2.09	2.09	2.54	5.47	1.76	1.76	2.21	4.70	1.81	1.81	2.27	–
V	1.76	1.76	2.15	4.69	–	–	–	–	–	–	–	–
VI	1.46	1.46	1.86	3.81	–	–	–	–	–	–	–	–

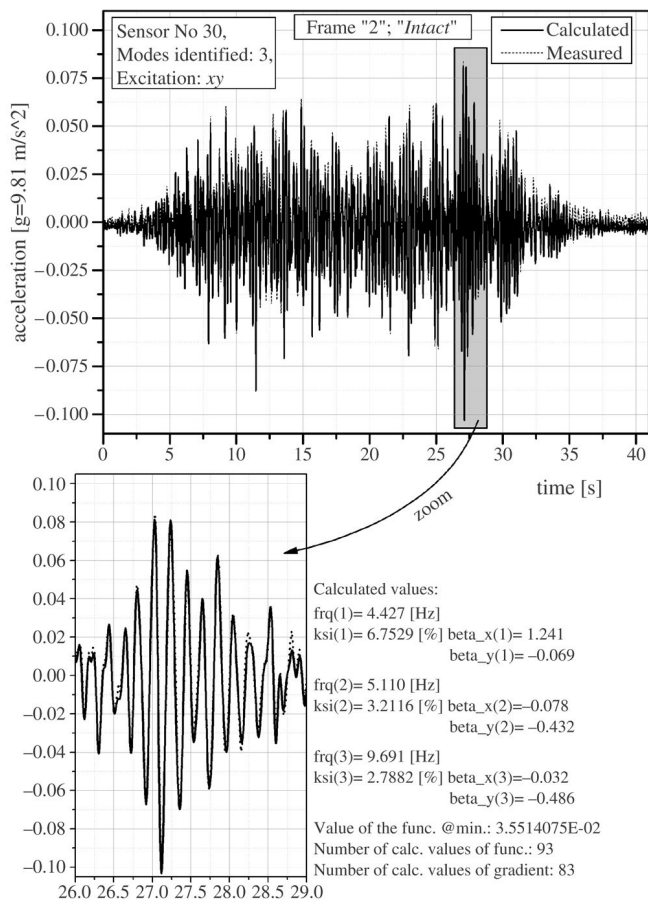


Fig. 12. Results of identification of intact frame 2 from time history records of excitation and response.

to note that with the level of damaging excitations described as “I” in Table 4 (PGV = 6.08 cm/s) the loss of frequency reached about 10% still without visual detection of cracks on the surface of the frame. This shows a good potential for the methods of damage detection in r/c structures based on measurements of changes in their natural frequencies. On the other hand, it can be seen from Figs. 19 and 20 that at least one additional level of excitation with PGV of about 8 cm/s should have been added to the sequence of experiments as it would show better the moment when the first cracks could be seen on the concrete surface. In Table 5 various approximations of the natural frequencies for frame 2 in progressive damage are shown. Not all the methods enabled identification of the

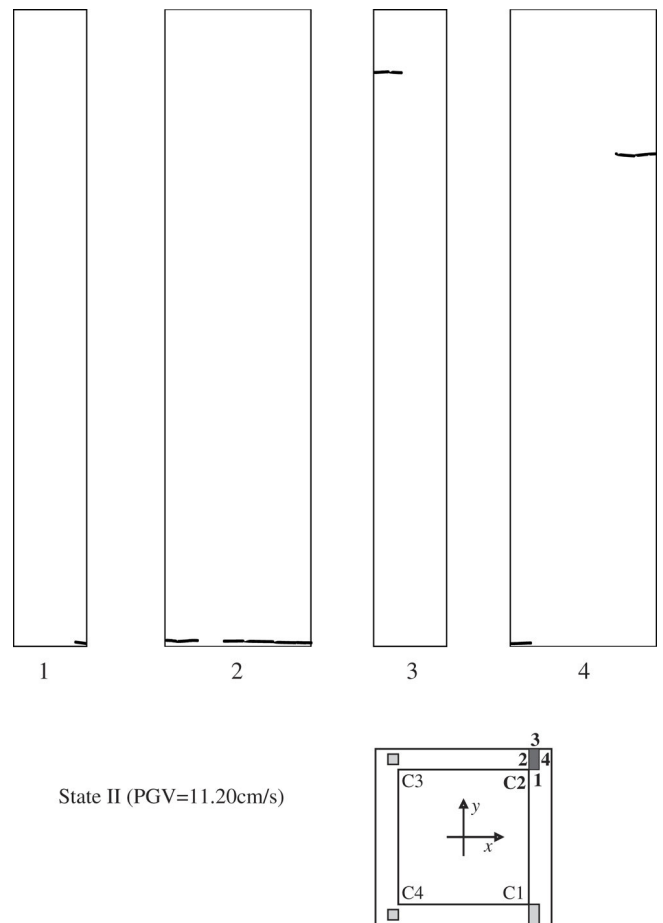


Fig. 13. Damage of column no. 2 of frame no. 2 after excitation at level of 6 dB (State II).

three, prominent natural frequencies. In particular the “seismic” identification which enabled identifying all three modes of intact frames failed to identify modes for the accelerometers not parallel to the identified mode as well as the torsion mode. All three modes in one run of the seismic identification algorithm could be identified only for intact (state N) and the first stage of damage (state I). Clearly the “seismic” algorithm should be further modified to properly take into account the non-linearities introduced in even low level vibrations by cracks made in the concrete.

When normalized to a common value of 100% at intact, the relative loss of natural frequencies revealed that the loss of

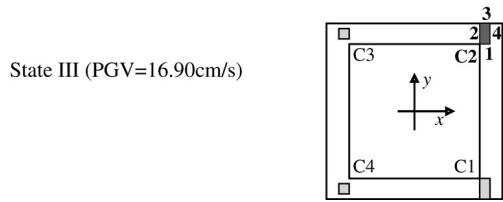
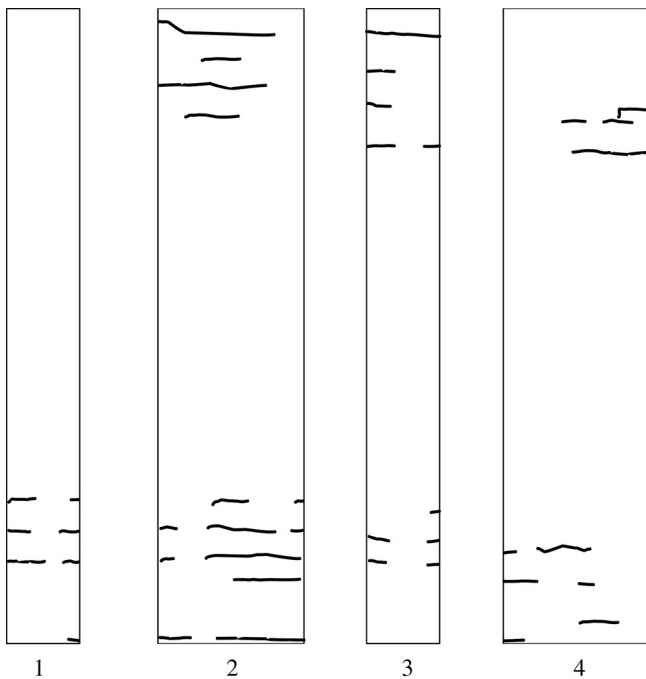


Fig. 14. Damage of column no. 2 of frame no. 2 after excitation at level of 9 dB (State III).

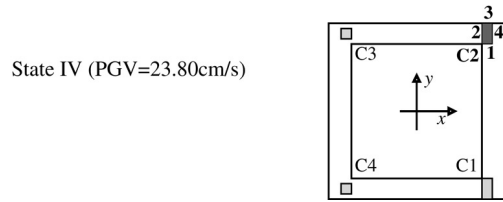
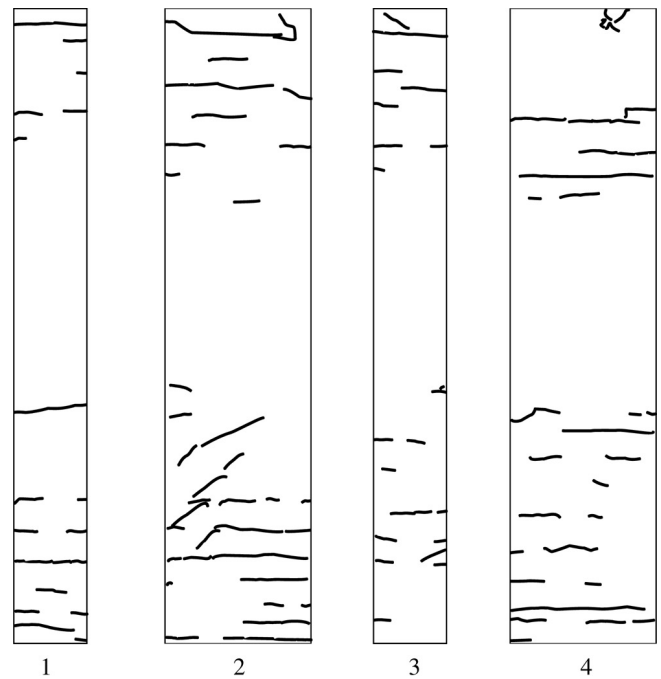


Fig. 15. Damage of column no. 2 of frame no. 2 after excitation at level of 12 dB (State IV).

frequency was the fastest for the first natural mode, slower for the 2nd mode and the slowest for the torsional mode as can be seen from Fig. 21. In this figure the shaded area indicates loss of natural frequencies not reflected by the visible presence of cracks.

The fall of natural frequencies with the increasing damage is a direct result of the bending stiffness loss for all the four columns. Since the damage was rather uniformly distributed among all the columns one may calculate the average loss of stiffness of the columns. This was done using a simplified, 3-dof model of the frame (Fig. 22). The equation of undamped, free vibrations of this system takes the following form:

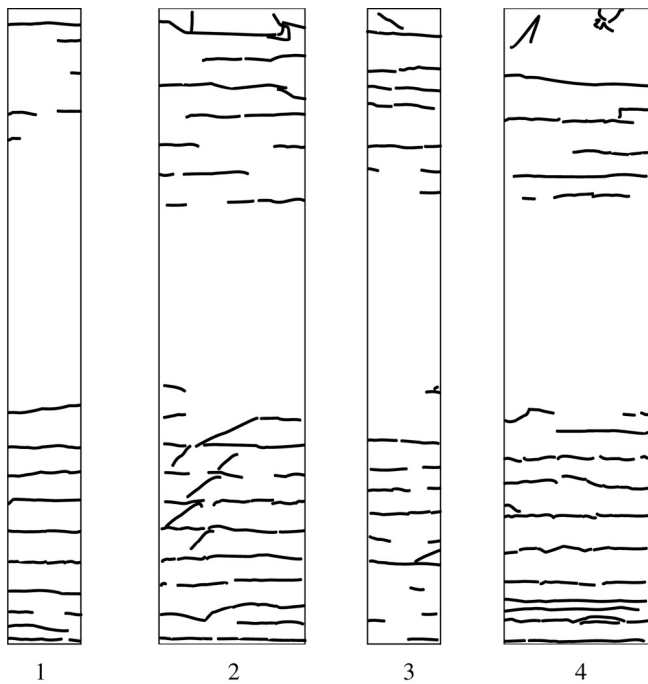
$$\mathbf{M}\ddot{\mathbf{q}} + \mathbf{K}\mathbf{q} = \begin{bmatrix} m & 0 & -em_d \\ 0 & m & em_d \\ -em_d & em_d & J_\varphi \end{bmatrix} \begin{bmatrix} \ddot{q}_x \\ \ddot{q}_y \\ \ddot{q}_\varphi \end{bmatrix} + \frac{EJ}{h^3} \begin{bmatrix} 72 & 0 & 0 \\ 0 & 216 & 84B \\ 0 & 84B & 54A^2 + 18B^2 \end{bmatrix} \begin{bmatrix} q_x \\ q_y \\ q_\varphi \end{bmatrix} = \mathbf{0} \quad (12)$$

in which m is the mass of the slab (including the additional mass m_d and half of the masses of the columns) and e is eccentricity of the mass m_d . Stiffness EJ is the smallest bending stiffness among all the columns (columns C3 & C4 from Fig. 22 and cross-section on the left in Fig. 3). As a result

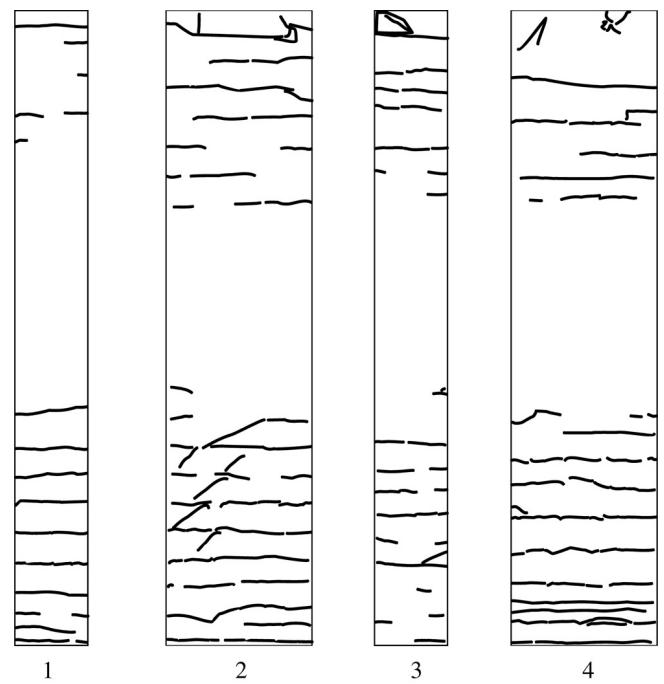
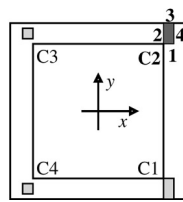
the stiffness matrix was formulated in terms of “comparative” stiffness EJ . The obvious simplification of this model derives not only from just 3-dof of this system, but also from the assumed fixed–fixed column boundary conditions in the slab and the lower spandrel. More detailed FEM computations revealed about 25% rotational flexibility of the upper end of the columns compared to about 2% rotational flexibility of their lower ends. This bias in column flexibility assumed for the simplified model of the structure from Fig. 22 (Eq. (12)) does not affect the proportions of the three natural frequencies of this system which are important to calculate average loss of column stiffness. In Fig. 23 the drop of “comparative” stiffness EJ is shown as a function of the damage inflicted to the structure. This drop was calculated by finding the best match of the first three measured natural frequencies with the ones obtained by solving Eq. (12). It was obtained by minimizing the following equation:

$$\sum_{i=1}^3 (f_i^m - f_i^c(EJ))^2 = \min, \quad i = x, y, \varphi \quad (13)$$

in which the superscript m stands for ‘measured’ natural frequencies while c stands for the calculated ones. From Fig. 23 about 15% drop of stiffness is observed before the cracks are visually detected.



State V (PGV=29.30cm/s)



State VI (PGV=38.20cm/s)

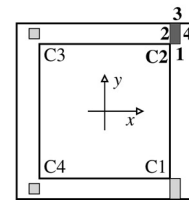


Fig. 16. Damage of column no. 2 of frame no. 2 after excitation at level of 14 dB (State V).

Fig. 17. Damage of column no. 2 of frame no. 2 after excitation at level of 16 dB (State VI).

Table 6
The values of MAC coefficients (damaged vs. intact frame)

		Experimental mode shapes (Intact state)			
		1	2	3	
Experimental mode shapes	State I	1	0.999	0.021	0.001
		2	0.010	0.981	0.005
		3	0.000	0.044	1.000
	State II	1	1.000	0.005	0.000
		2	0.020	0.920	0.002
		3	0.001	0.121	0.999
	State III	1	1.000	0.012	0.000
		2	0.017	0.923	0.001
		3	0.001	0.122	0.998
	State IV	1	0.999	0.009	0.000
		2	0.023	0.913	0.001
		3	0.001	0.133	0.997

As the full results of the sweep-sine tests were available for most of the damaged states, the eigenmodes at different states of damage were also analyzed. Their comparison with the ones from the intact state could not reveal clear differences except for a slight difference of the first mode at damage state IV (Fig. 24). This is also confirmed by the MAC values comparing the intact experimental eigenmodes with the experimental

modes obtained from sweep-sine tests for the damaged frame (Table 6).

The effect of damage on the structural damping was checked by the method of half power bandwidth from modulus of frequency response function either from random tests or sweep sine tests. However due to interaction of the analyzed frame with the system of actuators supporting the shaking table, substantial bias was introduced to such estimated damping ratios. The damping ratio ξ obtained this way equaled about 4.5% for the frame in intact state as compare with ξ about 2% obtained from impact tests when the shaking table was in fixed position (Table 3). Unfortunately, the impact tests which might properly reveal the evolution of damping could not be carried out during the damaging tests because the shaking table could not be moved down to rest position after each cycle of damaging excitations.¹ On the other hand even changes of such biased damping still revealed an increase in the damping ratio ξ which evolved from $\xi = 4.5\%$ in intact state to about 7%–9% when the structure was in the damage state VI (an increase of about 150%–200%).

¹ Moving the 6-dof shaking table from the rest to stand-by position required time consuming tuning procedures which would substantially increase the overall costs of the experiment.

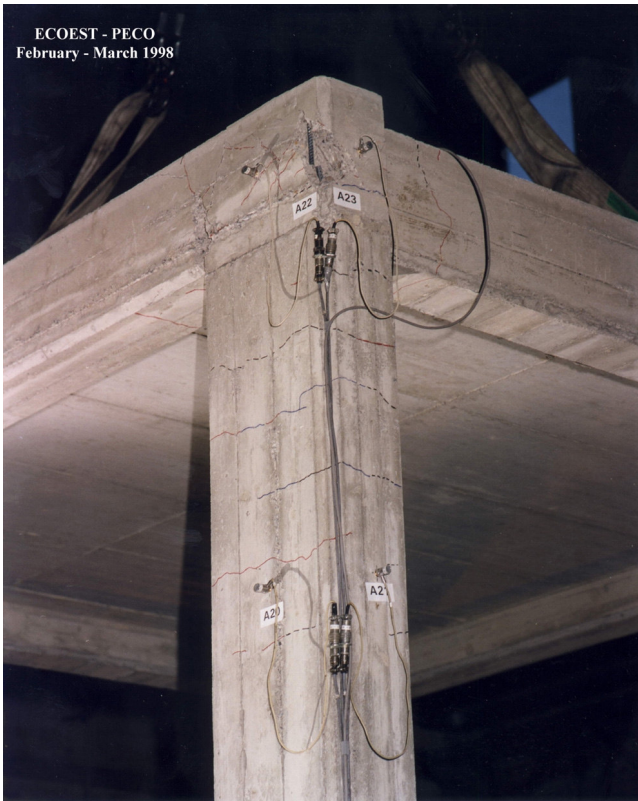


Fig. 18. Detail of damaged frame after seismic tests.

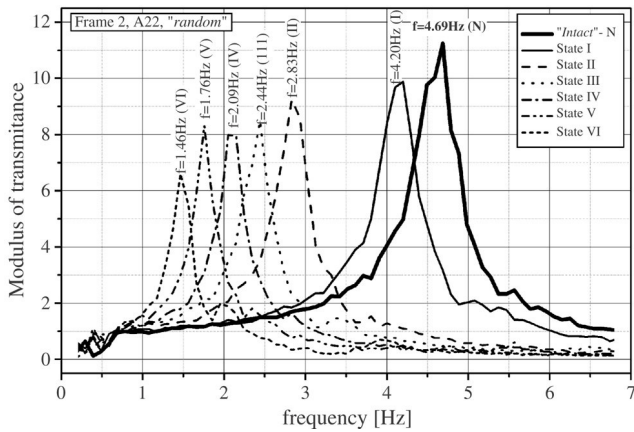


Fig. 19. The plot of transfer function between channel A30 and Ax obtained from random tests for various levels of excitation.

8. Discussion and conclusions

The results of a shaking table experiment aiming at full scale structural damage identification and modal analysis of reinforced concrete frames under progressive damage is presented. The observed reduction of stiffness of the analyzed reinforced concrete frames with the development of cracks is a well known phenomenon and the effects of these changes on dynamic properties of reinforced concrete structures are the subject of extensive, recent research to develop methods for non-destructive damage evaluation of r/c structures. The reported experiment had a similar purpose, testing, this

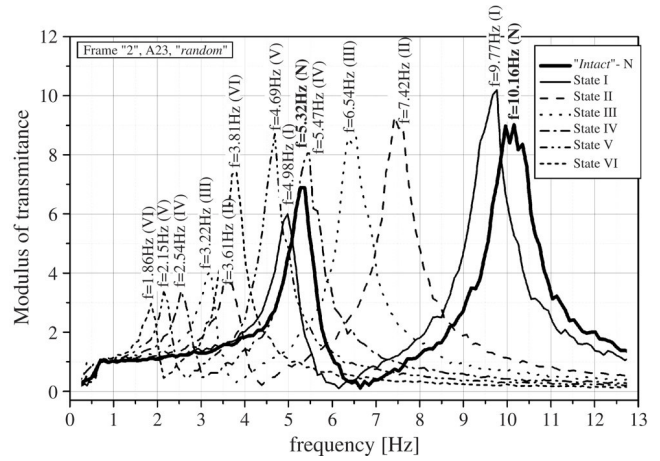


Fig. 20. The plot of transfer function between channel A23 and Ay obtained from random tests for various levels of excitation.

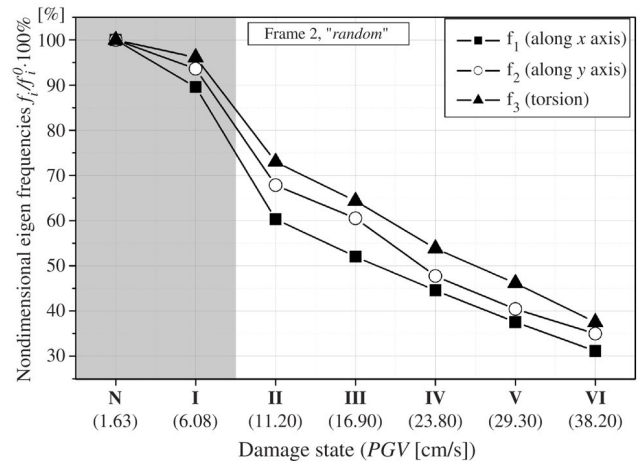


Fig. 21. Normalized natural frequency drop with progressive damage states (see Table 4).

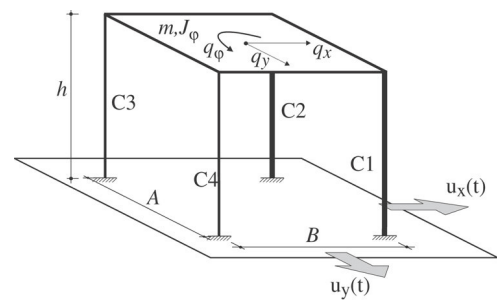


Fig. 22. Simplified 3-dof model of the frame.

time, full scale structures in the laboratory environment. The substantial loss of relative values of the natural frequencies was noted as expected. However this fall of natural frequencies was not uniform. It was fastest for the first natural mode, slower for the 2nd mode and the slowest for the torsional mode (Fig. 21). It was particularly interesting to note that the loss of natural frequencies reached about 10% and still the cracks could not visually be observed (respective loss of stiffness equaled 15%). This result is rather promising for the future applications of the non-destructive damage estimations of r/c

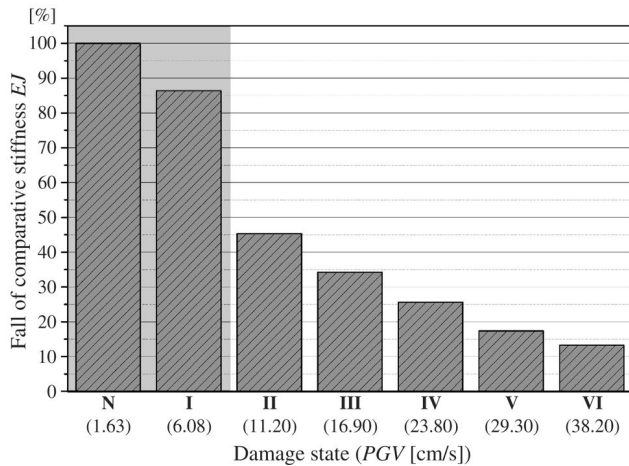


Fig. 23. Fall of comparative stiffness EJ with progressive damage states (see Table 4).

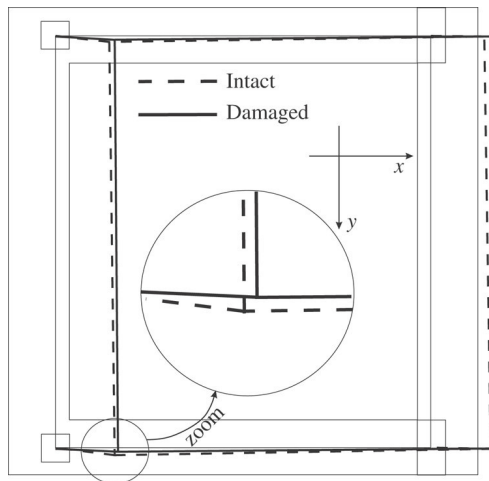


Fig. 24. Comparison of the first mode of vibration in intact state and damage state IV.

structures from their natural frequencies, since we can detect damage from vibrations before we could note it from ordinary inspections. The first part of damage accumulation, between the intact state and the appearance of the first cracks, proved to be particularly interesting so possible, future experiments should include more tests in this phase of the experiment. Substantial increase of damping could be observed during the experiment. Rather uniform distribution of damage from seismic, inertial forces among all four columns prevented however the natural modes to display clear differences in their shape with the loss of effective stiffness. Only a minor difference for the substantially damaged structure is indicated in Fig. 24.

Applying a shaking table for reinforced concrete, structural damage estimation enabled the full scale, heavy structure to be tested in a controlled, laboratory environment. This shaking table experiment revealed, however, also some difficulties and biases in the measurements deriving from the table–structure interaction effects. From this point of view the present results can particularly help planning and executing future identification experiments of r/c structures carried out on shaking tables.

Acknowledgements

The measurements utilised in this research were collected during a joint research project carried out in 1998 at ISMES, Bergamo, Italy and financed by ECOEST-PECO funds of European Commission. The active participants of the project were Stanislav Pospisil and Shota Uruszadze (Institute of Theoretical & Applied Mechanics Prague, Czech Republic), Hans Giese and Andreas Kayser (Wuppertal University, Germany) and Zbigniew Zembaty and Marcin Kowalski (Technical University of Opole, Poland). Partial support of Polish NSF Grant (Reg. Number: 8-T07E-008-20 in the years 2001–2002) is also gratefully acknowledged.

This paper was written in the Centre of Structural Integrity (CESTI) at the Technical University of Opole as part of its statutory activity supported by the European Commission (contract no. G1MA-CT-2002-04058).

References

- [1] Beck JL. Determining models of structures from earthquake records. Earthquake Engineering Research Laboratory, Report No.EERL78-01. Pasadena (CA): Caltech; 1978.
- [2] Bendat JS, Piersol AG. Engineering applications of correlation and spectral analysis. New York: John Wiley & Sons; 1980.
- [3] Castellani A. Concrete toughness after 20 years. Journal of Structural Engineering, ASCE 1992;118:1402–12.
- [4] Clough RW, Penzien J. Dynamics of structures. 2nd ed. New York: McGraw-Hill; 1993.
- [5] Dennis JE, Schnabel RB. Numerical methods for unconstrained optimization and nonlinear equations. New York: Prentice-Hall; 1983.
- [6] Doebling SW, Farrar CR, Prime MB, Shevitz DW. Damage identification and health monitoring of structural and mechanical systems from changes in their vibration characteristics: a literature review. Los Alamos National Laboratory Report LA-13070-MS. 1996.
- [7] Ewins DJ. Modal testing: theory and practice. New York: John Wiley & Sons; 1986.
- [8] Fletcher R. Practical methods of optimization. Chichester: John Wiley & Sons; 1987.
- [9] Franz G, Brener H. Verformungsversuche an Stahlbetonbalken mit hochfesten Bewehrungsstahl. Deutscher Ausschuss für Stahlbeton, H. 188/1967.
- [10] Jędrzejczak M, Knauff M. Flexural rigidity of RC elements with randomized concrete tensile strength. Archives of Civil Engineering 1997; 43(1):7–22.
- [11] Maeck J, De Roeck G. Dynamic bending and torsion stiffness derivation from modal curvatures and torsion rates. Journal of Sound and Vibration 1999;225(1):153–70.
- [12] Maia NMM, Silva JMM, He J, Lieven NAJ, Lin RM, Skingle GW et al. Theoretical and experimental modal analysis. Tauton (Somerset, UK): Research Studies Press Ltd.; 1997.
- [13] McVerry GH. Structural identification in the frequency domain from earthquake records. Earthquake Engineering and Structural Dynamics 1980;8:161–80.
- [14] Ndambi J-M, Vantomme J, Harri K. Damage assessment in reinforced concrete beams using eigenfrequencies and mode shape derivatives. Engineering Structures 2002;24(4):501–15.
- [15] Penzien J, Hansen RK. Static and dynamic elastic behavior of reinforced concrete beams. ACI Journal Proceedings 1954;50:545–67.
- [16] Salawu OS. Detection of structural damage through changes in frequency: a review. Engineering Structures 1997;19(9):718–23.
- [17] Sohn H, Farrar CR, Hemez FM, Shunk DD, Stinemas DW, Nadler BR. A review of structural health monitoring literature: 1996–2001. Los

- Alamos National Laboratory Report LA-13976-MS. 2003.
- [18] Trifunac MD, Brady AG. On the correlation of seismic intensity scales with the peaks of recorded strong ground motion. *Bulletin of the Seismological Society of America* 1975;65(1):139–62.
- [19] Wang Z, Man X-TC, Finch RD, Jansen BH. The dynamic behaviour and vibration monitoring of reinforced concrete beams. *Journals of Testing and Evaluation* 1998;26(5):405–19.
- [20] Wauer J. On the dynamics of cracked rotors: a literature survey. *Applied Mechanics Review* 1990;43(1):13–7.
- [21] Zembaty Z. Vibrations of bridge structure under kinematic wave excitations. *Journal of Structural Engineering, ASCE* 1997;123:479–88.
- [22] Zembaty Z, Kowalski M. Dynamic identification of a model of brick masonry building. *Archives of Civil Engineering* 2000;XLVI(1): 107–136.